

## Characterisation of suspended and sedimented particulate matter in blue-green infrastructure ponds

V. Krivtsov<sup>a,b,\*†</sup>, S. Arthur<sup>a</sup>, J. Buckman<sup>a</sup>, A. Kraiphet<sup>a</sup>, T. Needham<sup>c</sup>, Wanying Gu<sup>c</sup>, Prasuja Gogoi<sup>c</sup> and C. Thorne<sup>c</sup>

<sup>a</sup> Heriot-Watt University, Edinburgh, UK

<sup>b</sup> Edinburgh University, Edinburgh, UK

<sup>c</sup> Nottingham University, Nottingham, UK

\*Corresponding author. E-mail: vkritso@staffmail.ed.ac.uk

† Present address: RBGE, 20A Inverleith Row, Edinburgh EH3 5LR, UK

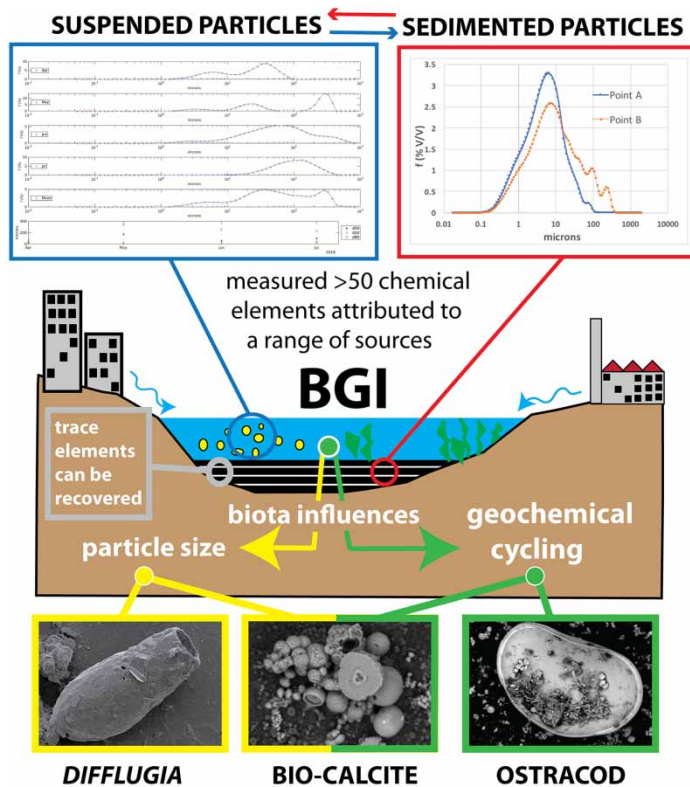
### Abstract

Blue-green infrastructure (BGI) ponds have an important function of alleviating flood risk and provide water quality improvements among other multiple benefits. Characterisation of bottom sediments and suspended particulate matter (SPM) is understudied, but is indispensable for assessing the ponds' functioning because of their role in biogeochemical cycling and pollutant adsorption. Here we report on the analysis of particle sizes and chemistry from multiple locations. The results have shown that SPM in these ponds includes particles of both biological and abiotic origin, and the *in situ* produced organic matter constitutes a major part of SPM. The relevance of biological processes is often overlooked, but a combination of scanning electron microscopy (SEM) observations and chemical analysis highlights its primary importance for characterisation of the particulate matter. A considerable proportion of both suspended and sedimented particulates is smaller than 100 microns. There is normally a large fraction of small silt-sized particles, and often a considerable proportion of very fine particles (clay-size). Although for some spectra unimodal distribution has been observed, in many cases the revealed particle size distribution (PSD) was bimodal, and in some instances more than two modes were revealed. A complex PSD would be expected to result from a combination of simple unimodal distributions. Hence the multimodality observed may have reflected contributions from different sources, both abiotic and biological. Furthermore, many smaller particles appear to be interconnected by detrital matter. Among chemical elements routinely detected within the SPM in significant concentrations were Si, Al, Ca, Mg, Fe, K, Mn, P, Cl and S. In a number of cases, however, there were less expected elements such as Ti, Y, Mo, Cr and even Au; these may have reflected the effect of car park and road runoff and/or industrial pollution. Most of these elements (except Mo and Au) and up to 30 others were also routinely detected in sediment samples. Such pollutants as Co, Cu, Ni, Zn and As were detected in bottom sediments of all ponds. There were a number of correlations between pollutants in sediments and the particle's median diameter. However, aggregation leads to large low density flocks and masks correlation of chemicals with SPM particle size. Statistical associations among the elements aided the understanding of their sources and pathways, as well as the underlying biological and abiotic processes. Specifically, our analysis implicated contributions from such sources as allochthonous and autochthonous detritus, roadside and industrial pollution, biologically induced precipitation, and discarded electronics. Elevated levels of rare earth elements (REE) and other trace elements open a possibility of their recovery from the sediments, which should be considered among the multiple benefits of BGI.

This is an Open Access article distributed under the terms of the Creative Commons Attribution Licence (CC BY 4.0), which permits copying, adaptation and redistribution, provided the original work is properly cited (<http://creativecommons.org/licenses/by/4.0/>).

**Key words:** biological mediation, coprecipitation, geochemical cycling, particle size, REE, resource recovery

## Graphical Abstract



## INTRODUCTION

Ponds are an important part of the blue-green infrastructure (BGI) network and are routinely used in urban environments for enhancing flood resilience. In particular, sustainable urban drainage systems (SUDS) retention ponds are specifically designed to alleviate flood risk. BGI ponds have a hydrological storage function, which opens possibilities for usage of stormwater as a resource (Fenner *et al.* 2019; O'Donnell *et al.* 2020). BGI ponds also provide water quality improvements (Arthur *et al.* 2019) and other ecosystem services, as well as multiple social benefits related to their educational and recreational values (Krivtsov *et al.* 2020). Characterisation of suspended particulate matter (SPM) and bottom sediments is indispensable for assessing a pond's functioning because of their role in biogeochemical cycling and pollutant adsorption (Krivtsov *et al.* 2019b).

Many previous studies have examined relationships between particle sizes and pollutants adsorption in SUDS ponds, and a review is available in a recent CIRIA report (Arthur *et al.* 2019). However, due to the costs involved, the number of considered elements is usually limited and biological processes are often overlooked. Typically, the inclusion of a limited number of chemical elements (restricted by financial and logistical constraints) is justified by their known toxicity in the aquatic environment and the expectation of encountering elevated concentrations due to the known pollution sources. Consequently, occurrence, interactions and biogeochemical cycling of many elements remain largely unexplored.

However, geochemical cycles in aquatic systems are interconnected, and simultaneous consideration of multiple elements contributes to a better understanding of their connections, interrelated direct and indirect effects, and implications for the overall ecological functioning (Krivtsov 2004,

2008; Krivtsov *et al.* 2000b; Zavarzin 2002, 2008). Thus, a more comprehensive characterisation of SPM and bottom sediments is beneficial for enhancing our understanding of sources, pathways and processes involved. In particular, consideration of trace elements is important because of their potential limiting role for primary production and the dynamics of microbiological community (Reynolds 1984, 2006), as well as the potential to bioaccumulate in plants and higher trophic levels (Zayed *et al.* 1998; Nelson *et al.* 2000). There are also potential economic considerations as regards rare earth elements (REE), whose global usage has increased dramatically in the last 15 years (Migaszewski & Gałuszka 2015). REE are increasingly widely used in medical industry, as well as in permanent magnets and electronics (Humphries 2013). Other widespread applications include the use in glass additives, polishing compounds, pigments, rechargeable batteries, energy saving lamps, mobile phones, and in catalytic converters in cars (Migaszewski & Gałuszka 2015). Airborne particulates originated from fossil fuel combustion have been reported to contribute to the elevated REE levels in waters, soils and biota (Migaszewski & Gałuszka 2015). Previous research looked into a possibility of economic recovery of REE from wetlands constructed to remove pollutants from industrial effluent (Schaller *et al.* 2013), but the BGI ponds have not yet been considered in that regard.

Total concentrations of suspended solids are routinely reported in monitoring and experimental studies of SUDS ponds, and the measured levels of small particles are often used as a proxy for other pollutants (Allen 2017; Allen *et al.* 2017; Arthur *et al.* 2019). However, a more detailed characterisation of SPM is scarce, and to our knowledge scanning electron microscopy (SEM) and X-ray techniques have not yet been applied for this purpose. In modelling research, SPM is also treated as a 'black box' (Ahilan *et al.* 2019). The simulation models tend to include only a limited selection of particle sizes (and usually just the average or the most predominant size). Hence the potential complexity of the spectra is not considered by the existing models.

The research presented here combines the application of X-ray based techniques capable of simultaneous detection of a comprehensive range of elements with SEM observations, traditional gravimetric measurements of suspended solids and loss on ignition (LOI) measurements identifying their separate fractions. It aims to improve characterisation of suspended and sedimented particulate matter in urban BGI systems, which will enhance our understanding of their biogeochemistry and overall functioning and will therefore contribute to the developments of their design and management practices. This is of relevance for water quality monitoring and modelling, for estimation of elemental budgets and throughputs, for further studies on planktonic and benthic microbiological communities, and may also have implications for the risk assessment of water-borne diseases. The results, therefore, will be of value for planning of BGI network assets within the wider urban flood resilience (UFR) and blue-green cities (BGC) conceptual framework (Fenner *et al.* 2019; O'Donnell *et al.* 2020).

---

## METHODS

Here we report on the study of bottom sediments and suspended particulate matter at nine BGI ponds located around Edinburgh and Lothians (Scotland, UK). Unless indicated otherwise, each pond was sampled at two points, with samples denoted as 'A' and 'B'. Typically, those sampling points were positioned at the opposite parts of the ponds. Most of the ponds are located in typical urban catchments characterised by the predominance of impervious surfaces. However, the catchments of the RBGE, Blackford and Gore Glen ponds are predominantly pervious and covered by vegetation dominated by mature trees. Further information about the sites, including the data on area, age, and vegetation, is given elsewhere (Krivtsov *et al.* 2019b). Data from other locations (Gogoi 2018) were also used in statistical analysis on the enhanced dataset.

For particle size measurements of SPM, the water samples collected from the ponds were analysed using a Mastersizer S instrument (Malvern Panalytical, <https://www.malvernpanalytical.com/en>). For

SPM chemical analysis, the water samples were filtered through polycarbonate filter membranes, and the deposited particulates were analysed using SEM combined with energy dispersive X-ray (EDX) analysis (Quanta FEG 650, with Oxford Instruments X-Max<sup>N</sup> 150 mm detector). The data were processed using AZtec software. The quantitative detection limit of the method used is ~0.1 wt% (Oxford Instruments 2013, 2019). However, the limit is variable and depends on the amount of material and properties of the matrix, background values, and the combination of analytical parameters. Where the estimated concentration is higher than the corresponding detection limit, the AZtec software reports results in yellow colour; however, in some cases the software lists the estimates of concentrations in red, which provides only an indication of an element's presence (Oxford Instruments 2013, 2019). Typically, the red listings happen when the separation of the elemental peaks could not be reliably resolved, and/or when the very low quantity precludes an accurate estimate. These instances are reported as '+' (i.e. presence) in Table 1.

Particle size distribution for the sediment samples was undertaken using a Beckman Coulter LS13 320 Laser Diffraction Particle Size Analyser. Prior to the analysis, hydrogen peroxide was added to the samples and heated to 80 °C to remove the organic materials from the sediments. The samples were centrifuged, the peroxide solution was decanted off and the sediment re-suspended by shaking for a minute in distilled water. This process was repeated three times so that all the peroxide and any residual organic material was removed. The sediment was finally re-suspended in a 10% calgon solution to prevent aggregation of finer particles. The suspended sediment sample was introduced to the fluid module of the laser particle size analyser and passed through a laser beam; detectors placed at fixed angles measure the intensity of light scattered at that position. The sample d50 and particle size distribution were recorded for each sample.

Chemical concentrations of selected elements in the sediment samples were measured using XRF spectroscopy. This method is based on an analytical technique that exposes a solid sample to an X-ray source. The X-rays from the source have that suitable excitation energy that causes elements in the sample to emit characteristic X-rays. A Panalytical Epsilon 3-XL XRF analyser used in this study consists of three major components:

1. The source that generates X-rays (an X-ray tube with a silver target anode).
2. An energy dispersive, solid state detector that converts X-rays emitted from the sample into measurable electronic pulses.
3. A data processing unit that records the fluorescence energy signals and calculates the elemental concentrations in the sample (Brouwer 2006).

The detection limits of the XRF technique used for the analysis of sediments is 0.001% dwt. It should, however, be noted that the XRF technique does not detect the elements in the first two rows of the periodic table (H–Ne). Also, detection of any elements after U is unreliable. Furthermore, the method may not be suited for the detection of noble gases.

Correlation and factor analyses were used to reveal statistical associations among elements within SPM and bottom sediments. These methods were previously used for similar purposes by other studies (Krivtsov *et al.* 1999a, 1999c).

---

## CHARACTERISATION OF SPM IN THE PONDS STUDIED

### Size distribution of suspended particulate matter

The results show that particle size distribution (PSD) is dynamic and changes throughout the study period (Figure 1). Two interesting features can be seen in the spectra. Firstly, a considerable (and often the major) proportion of SPM in all the ponds was represented by particles <100 microns.

**Table 1** | Average SPM elemental concentrations (mg/kg dwt)

| Pond/element | Appleton | Blackford | Botanics | Eliburn | Gore Glen | Granton | Inverleith | Juniper Green | Oxgangs |
|--------------|----------|-----------|----------|---------|-----------|---------|------------|---------------|---------|
| Al           | 240      | 169       | 136      | 295     | 226       | 143     | 365        | 194           | 334     |
| As           | +        | NF        | NF       | NF      | NF        | +       | +          | NF            | NF      |
| Au           | NF       | NF        | NF       | NF      | NF        | NF      | NF         | 16            | NF      |
| B            | NF       | NF        | NF       | NF      | +         | NF      | NF         | NF            | NF      |
| Ba           | NF       | +         | +        | +       | 4         | +       | 5          | NF            | +       |
| Br           | +        | 15        | +        | 6       | 2         | +       | +          | 15            | 0       |
| Ca           | 229      | 509       | 207      | 99      | 263       | 1,168   | 318        | 1,035         | 286     |
| Cl           | 26       | 15        | 0        | +       | +         | +       | +          | +             | +       |
| Cr           | 38       | 53        | 8        | 4       | 6         | 19      | 21         | 59            | +       |
| Dy           | NF       | NF        | NF       | NF      | NF        | NF      | NF         | NF            | NF      |
| Er           | NF       | NF        | +        | NF      | NF        | +       | +          | NF            | NF      |
| Eu           | NF       | NF        | NF       | NF      | +         | NF      | +          | NF            | NF      |
| F            | NF       | NF        | NF       | NF      | NF        | NF      | NF         | NF            | NF      |
| Fe           | 473      | 911       | 604      | 233     | 615       | 326     | 1,146      | 3,005         | 496     |
| Ge           | +        | NF        | NF       | NF      | NF        | +       | +          | NF            | NF      |
| Hf           | NF       | NF        | NF       | NF      | NF        | +       | NF         | NF            | NF      |
| Hg           | NF       | NF        | NF       | NF      | NF        | NF      | NF         | NF            | NF      |
| Ho           | NF       | NF        | NF       | NF      | NF        | NF      | NF         | NF            | NF      |
| I            | NF       | NF        | +        | NF      | NF        | NF      | NF         | NF            | NF      |
| In           | +        | NF        | +        | NF      | NF        | +       | +          | NF            | +       |
| Ir           | +        | +         | +        | NF      | +         | +       | +          | +             | NF      |
| K            | 36       | 32        | 44       | 58      | 42        | 30      | 59         | 16            | 51      |
| Mg           | 41       | 70        | 421      | 58      | 39        | 46      | 122        | 10            | 49      |
| Mn           | 69       | 133       | 775      | 88      | 282       | 207     | 148        | 116           | 187     |
| Mo           | +        | +         | +        | 6       | 1         | +       | 20         | +             | 3       |
| Na           | 32       | 40        | 3        | 2       | 9         | 2       | 4          | +             | 15      |
| Ni           | 14       | 8         | 4        | +       | 4         | +       | +          | +             | +       |
| Os           | +        | NF        | NF       | NF      | NF        | NF      | NF         | NF            | +       |
| P            | 34       | 175       | 51       | 73      | 36        | 113     | 352        | 39            | 80      |
| Pr           | +        | NF        | NF       | NF      | NF        | NF      | NF         | NF            | NF      |
| Rb           | +        | NF        | +        | NF      | +         | NF      | +          | 1             | +       |
| S            | 47       | 61        | 90       | 32      | 132       | 67      | 56         | 177           | 43      |
| Sb           | NF       | NF        | +        | NF      | NF        | 19      | NF         | +             | NF      |
| Si           | 880      | 1,190     | 1,910    | 609     | 692       | 633     | 1,335      | 861           | 1,121   |
| Sn           | NF       | NF        | NF       | NF      | NF        | NF      | NF         | NF            | NF      |
| Sr           | NF       | +         | +        | +       | +         | 2       | NF         | 2             | +       |
| Ta           | NF       | NF        | NF       | NF      | NF        | NF      | +          | NF            | NF      |
| Tb           | NF       | NF        | NF       | +       | NF        | NF      | NF         | NF            | NF      |
| Te           | NF       | NF        | NF       | NF      | NF        | NF      | NF         | NF            | +       |
| Ti           | 6        | 4         | 4        | 7       | 17        | 4       | 21         | 4             | 14      |
| Tl           | NF       | NF        | NF       | NF      | NF        | NF      | NF         | NF            | NF      |
| Tm           | NF       | NF        | +        | NF      | +         | 0       | NF         | NF            | NF      |
| U            | NF       | NF        | NF       | +       | NF        | NF      | NF         | NF            | NF      |
| V            | NF       | NF        | NF       | NF      | NF        | NF      | NF         | NF            | +       |
| W            | +        | +         | +        | +       | +         | +       | +          | 5             | +       |

*(continued)*

**Table 1** | continued

| Pond/element | Appleton | Blackford | Botanics | Eliburn | Gore Glen | Granton | Inverleith | Juniper Green | Oxgangs |
|--------------|----------|-----------|----------|---------|-----------|---------|------------|---------------|---------|
| Y            | 2        | +         | +        | +       | NF        | +       | NF         | 13            | NF      |
| Yb           | +        | NF        | +        | NF      | NF        | +       | +          | NF            | +       |
| Zn           | +        | NF        | +        | +       | NF        | +       | +          | +             | 3       |
| Zr           | NF       | NF        | NF       | NF      | NF        | +       | NF         | NF            | NF      |

'NF': no indication of the element's presence was found.

'+' : there was an indication of the element's presence, but the reliable estimate of concentration could not be given (red measurements only).

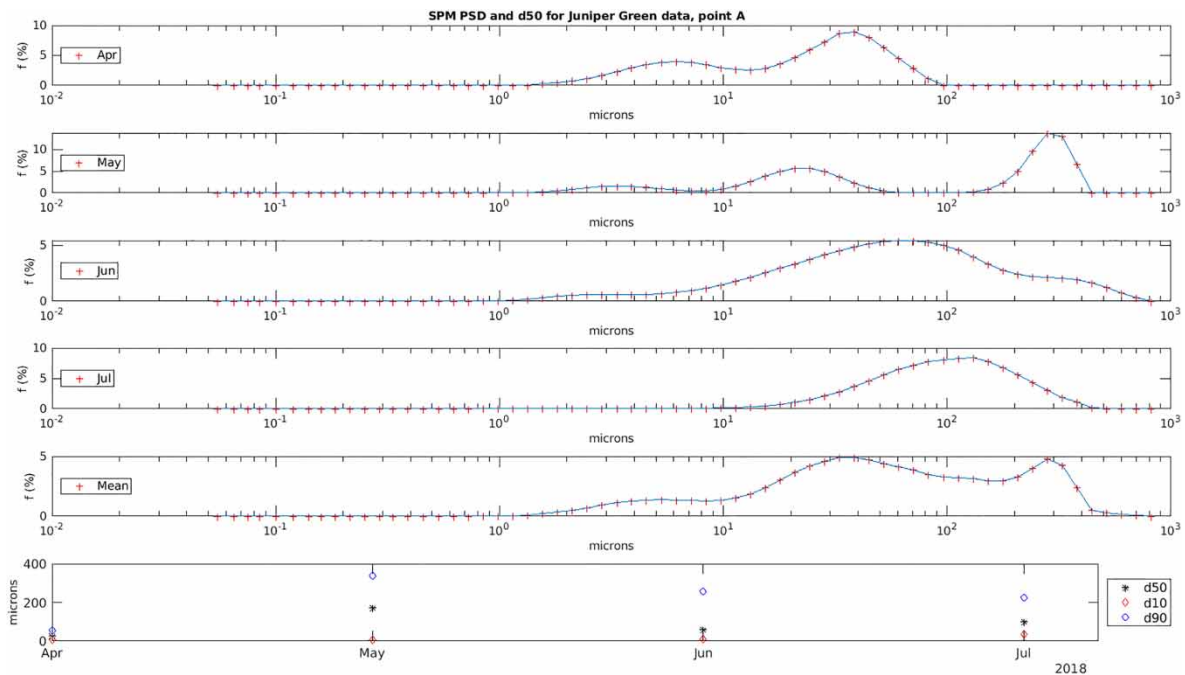


**Figure 1** | Example of particle size distribution of SPM data: temporal changes at Juniper Green pond (sampled at point A). Note temporal differences in PSD spectra, with unimodality in July and multimodality in May.

There is normally a large fraction of small silt-sized particles and often a considerable proportion of very fine particles (clay-size). The abundance of fine particles has implications for adsorption of nutrients and pollutants, and is therefore relevant for biogeochemical cycling and for water quality (Ma & Singhirunnusorn 2012; Zafra *et al.* 2017).

Secondly, although for some spectra unimodal distribution has been observed, in many cases the revealed PSD was bimodal, and in some instances more than two modes were revealed. The majority of the samples appear to have unimodal spectra. However, in April 2018, most of the spectra studied were characterised by bimodal distribution. For example, Juniper Green had bimodal spectra in May (Figure 1), whilst both Appleton and Eliburn had at least one bimodal spectrum in April, May and June 2018. A complex PSD would be expected to result from a combination of simple unimodal distributions. Hence the multimodality observed may have reflected contributions from different sources, both abiotic and biological (Krivtsov *et al.* 2008b). Furthermore, the PSD spectra are not static, but rather change between different sampling visits, thus reflecting the concurrent conditions, which is in line with previous studies elsewhere (Krivtsov *et al.* 2009). Temporal changes in spectral shape may have been influenced by progressive accumulation of polysaccharides and other compounds exuded by biological organisms (Tien *et al.* 2002). It should also be noted that PSD of SPM in aquatic systems is influenced by a number of interlinked processes, including sedimentation, resuspension,

precipitation, dissolution, flocculation and disaggregation (Krivtsov *et al.* 2008b). In the current study, both light and electron microscopy revealed interactions between microbiota and SPM.

There are a number of factors which may have influenced the exact shape of distribution, including for example inputs from the catchment, turbulence, and biological activity within the system (Krivtsov *et al.* 2008a, 2008b, 2009). Given that the majority of suspended particulates are organic (data not shown), the biological community of the ponds studied appears to be a major factor influencing the PSDs obtained. This influence would have been both direct, i.e. due to the relative abundance of specific species (Krivtsov *et al.* 2019b) and indirect (e.g. due to precipitation of chemicals, including calcite, following biologically induced changes in pH), as well as flocculation due to the production of polysaccharides (see Krivtsov & Sigeo 2005; Krivtsov 2008; Krivtsov *et al.* 2009 and references therein). Big flocks have been observed in a BMP pond previously (Marsalek *et al.* 2002), and were characterised by low density, low settling velocity and high contamination levels.

### Chemistry of suspended particulate matter

The summary of results (expressed in ppm) is given in Table 1. Both organic and inorganic particles have been commonly observed, and many of the smaller particles appear to be interconnected by detrital matter. Among chemical elements routinely detected within the SPM in significant concentrations were C, O, Si, Al, Ca, Mg, Fe, Mn, P, Cl and S. In a number of cases, however, there were less expected elements such as Ti, Y, Mo, Cr and even Au; these may reflect the effect of car park and road runoff and/or industrial pollution. For example, Cr inputs to stormwater are well known (Arthur *et al.* 2019) and may result from wearing out of vehicle tyres and brake pads; the element is also used in paints (Sörme & Lagerkvist 2002; Wei & Yang 2010). Ti also originates from the degradation of brake linings and tyres (Sternbeck *et al.* 2002; Thorpe & Harrison 2008), and has previously been recorded in urban stormwater in concentrations up to 37  $\mu\text{g l}^{-1}$ . The inputs of Y and Au are likely from discarded electronics, whilst Mo from airborne particulates (Hong *et al.* 2012).

Occasionally encountered in the samples were fragments of silicates (feldspar and quartz). P appeared to have tendency to be associated with Ca and/or with biologically derived detritus, whilst S was mostly associated with Fe (pyrite), but also appeared to be present in other forms (possibly elemental S).

An interesting feature observed at all sites is the scarcity of Gd in the SPM samples, despite its relative abundance in the sediments (see below). This element is not readily adsorbed to organic and clay particles and may therefore be expected to stay in the dissolved phase within the water column (Kulaksız & Bau 2011, 2013).

### Statistical analysis on the SPM chemical variables

Factor analysis, as well as Spearman correlation analysis were used to elicit the relationships of SPM chemicals. Due to the insufficient quality or quantity of data, the following elements were excluded from this analysis: As, Dy, F, Hf, Hg, Ho, I, Ta, Tb, Tl, Ge, Os and Sn. For correlation analysis the data on elemental concentrations were combined with subjective estimates of abundances of detritus, biota, and the common minerals (calcite, feldspar and other types of silicates), as well as measurements of particle sizes and concentrations of suspended solids. For brevity, the full results of correlation analysis are not shown (the majority of relationships were not significant), but the significant correlations are noted below in the text.

A number of elements (Al, Ba, Ca, Mg, P, Si, Ti, S) and the abundance of particles comprised of silicate minerals revealed significant positive correlations with total suspended solids (TSS) as well as with their organic and inorganic fractions. W and Cl, however, showed significant relationships only with TSS, whilst Na did with both TSS and the organic fraction. Interestingly, calcite correlated

only with the organic fraction, and did not show significant relationships with either TSS or the inorganic fraction. The absence of correlation with the inorganic fraction may be explained by low quantities of calcite and other inorganic compounds in the samples. The correlation with the organic fraction, however, is indicative of biologically induced precipitation of calcite, which was observed by visual inspection of SEM micrographs (Figure 2).

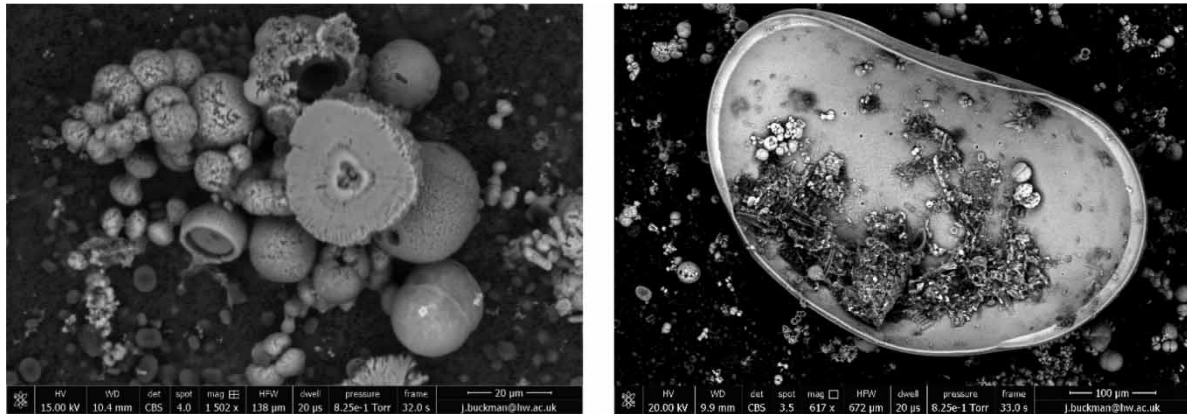


**Figure 2** | Spheroidal inorganic calcite deposits (left) and an ostracod shell (right) from Granton B sample in July.

TSS and their specific fractions showed no significant correlations with the subjectively estimated abundance of algae and diatoms but were positively related to the abundance of other biological organisms. Fe showed a positive correlation with detritus and negative with protozoa. P, S, Tm, Yb and Mn showed positive correlations with the abundance of biological organisms, whilst Rb revealed a negative relationship with the abundance of ‘other organisms’ and Mo with the abundance of algae. It should be noted, however, that the peaks of Mo and S are hard to differentiate, and the latter result therefore should be treated with caution.

Y revealed a negative correlation with median diameter, which can be explained by its preferential adsorption to smaller particles. Median diameter also negatively correlated to the abundance of diatoms and silicates (some of which were possibly of broken frustules origin).

Au positively correlated with the abundance of ferrosilicates whilst U with feldspar and silica, and Zn with silicates. W was correlated with silicates and calcite, whilst Y and Zn with aluminosilicates, and V with feldspar.

All in all, the correlations observed have variously highlighted the importance of both biological and abiotic processes in influencing the chemical properties of SPM. Further insight was gained by application of factor analysis.

Five factors extracted using factor analysis (Table 2) explained 51.87% of the variance observed. Factor 1, accounting for over 18.8% of the variance, had high loadings on most of the major elements (Al, Fe, K, Mg, Na, P, S and Si) except Ca and Mn, and is therefore likely to have reflected the importance of detritus. As our microscopy observations confirmed, the detritus in the SPM is of a mixed origin, and that is reflected in loadings of specific elements. High loadings of Al and Fe reflect the inorganic contribution; high loadings of P and S are due to the organic source, whilst Si would have reflected both inorganic (from aluminosilicates in sand and clay particles) and biological (from diatoms) origin. Association of Ti with this factor is likely due to the contribution of roadside or industrial pollution.

Factor 2 explained almost 11.5% of the variance observed in the data. It had high loadings on Ca and Zr, and may have reflected the contribution of particles originated from weathering of building materials. However, given our observations of biologically precipitated Calcite (see below), this factor is also likely associated with microorganisms’ influences, and high loadings on Tm may have



**Table 2** | Results of factor analysis (absolute loadings >0.5) on the SPM elements

| Elements | Components |       |       |       |       |
|----------|------------|-------|-------|-------|-------|
|          | 1          | 2     | 3     | 4     | 5     |
| Al       | 0.942      |       |       |       |       |
| Au       |            |       |       | 0.861 |       |
| B        |            |       | 0.639 |       |       |
| Ba       | 0.570      |       |       |       |       |
| Ca       |            | 0.955 |       |       |       |
| Cr       |            |       | 0.696 |       |       |
| Er       |            |       |       |       | 0.709 |
| Fe       | 0.845      |       |       |       |       |
| Ir       |            |       |       | 0.927 |       |
| K        | 0.876      |       |       |       |       |
| Mg       | 0.870      |       |       |       |       |
| Mo       |            |       |       |       | 0.701 |
| Na       | 0.538      |       |       |       |       |
| Ni       |            |       | 0.767 |       |       |
| P        | 0.538      |       |       |       | 0.517 |
| S        | 0.766      |       |       |       |       |
| Si       | 0.921      |       |       |       |       |
| Ti       | 0.923      |       |       |       |       |
| Tm       |            | 0.968 |       |       |       |
| Y        |            |       |       | 0.947 |       |
| Yb       |            | 0.935 |       |       |       |
| Zr       |            | 0.977 |       |       |       |

Extraction method: principal component analysis. Rotation method: Varimax with Kaiser normalization.

resulted from co-precipitation. Factor 2 also had high loadings on Yb. However, false Yb peaks may be produced in association with Ca in calcite, as Yb has an X-ray energy exactly double that of the main Ca peak. When two main Ca X-rays hit the detector at the same time, they produce a sum peak at the Yb position; this result therefore should be treated with caution.

Factors 3 and 4 each explained about 7.7% of the variance observed. Factor 3 had high loadings on Cr and Ni and is therefore associated with heavy metal pollution, likely of mixed origin. Factor 4 had high loadings on gold, iridium and yttrium. It is likely that this factor has reflected the presence of discarded electronics and/or other technological equipment.

Finally Factor 5, explaining a relatively lower proportion of variance (6.15%) may be reflecting adsorption of Er and Mo on P compounds. Due to the scarcity of other loadings, this factor is not well characterised but may have reflected adsorption of Mo to the exterior of some unidentified linear objects (possibly of biological origin), which was observed in some samples. Also, as has already been pointed out, there are problems in separation of Mo and S peaks, hence the statistical relationships revealed by Mo should be treated with caution.

The results of statistical analysis presented in this section implicate a mixed origin of SPM, with contributions from a range of sources, including weathering of building materials, allochthonous and autochthonous detritus, roadside and industrial pollution, biologically induced precipitation, and discarded electronics. The relevance of biological community is further discussed in the next section. Future research should investigate fine details of biological and chemical transformations of SPM in these and other BGI ponds.

### Relevance of the biological community

Biological organisms influence chemistry of SPM in a number of ways. Firstly, they exude organic compounds which then bind metals and metalloids (Tien *et al.* 2002; van Leeuwen & Buffle 2009) and coat the particles aiding flocculation (Krivtsov *et al.* 2008b; Krivtsov *et al.* 2009). Secondly, they take and adsorb chemicals which then follow these organisms' life cycles, typically resulting in the spatial redistribution and compartmentalisation (Krivtsov & Sigeo 2005). Thirdly, microorganisms may also increase interactions of trace elements with minerals (Perelomov & Kandeler 2006; Perelomov & Yoshida 2008) and lead to co-precipitation of trace elements with other compounds (Migaszewski & Gałuszka 2015). All these mechanisms appear to be relevant in the current study.

Application of SEM for direct observation allowed us to gather evidence for a mediating role of biological community in coprecipitation of inorganic compounds. These instances were registered both in SUDS ponds (Oxgangs, Granton) and in other BGI ponds (Gore Glen). For example, as has already been noted, the abundance of calcite correlated with the organic fraction of suspended solids. In line with that, observational analysis of SEM micrographs has shown that in Granton (point B) and RBGE (point B) July 2018 samples, there were amalgamated spheroidal inorganic mineral deposits enriched in Ca (Figure 2) co-occurring with high number of small organic particulates, likely of bacterial origin. The latter particles were present at both ends of the pond, but the inorganic precipitates were only observed at point B. It is therefore likely that the inorganic precipitates were forming *in situ* there (they would have been disaggregated by transportation otherwise) and have also been influenced by variation in water chemistry. The point B sample from Granton also contained an ostracod shell (Figure 2). Hence there was enough Ca to construct the shell, and excess to allow bacterial precipitation of  $\text{CaCO}_3$  as well. These processes were only occurring at one end, possibly reflecting more stagnant conditions there. Biologically induced coprecipitation of calcite has been previously studied in both brackish (Busquets *et al.* 2014) and natural freshwater (Dittrich & Obst 2004) environments, but this is the first time that this process has been observed in SUDS ponds.

Another example of biological mediation of SPM dynamics relates to the occurrence of testate amoeba (Figure 3). Most of the examples of testate amoeba were observed in the Gore Glen BGI pond, but they were also registered in Appleton, Granton, Juniper Green and Oxgangs SUDS ponds. The more commonly occurring species (*Diffflugia*) have tests covered in detrital grains (thus taking detrital particulates out of circulation), whilst others such as *Trinema* (less common) having secreted siliceous discs (Figure 3).

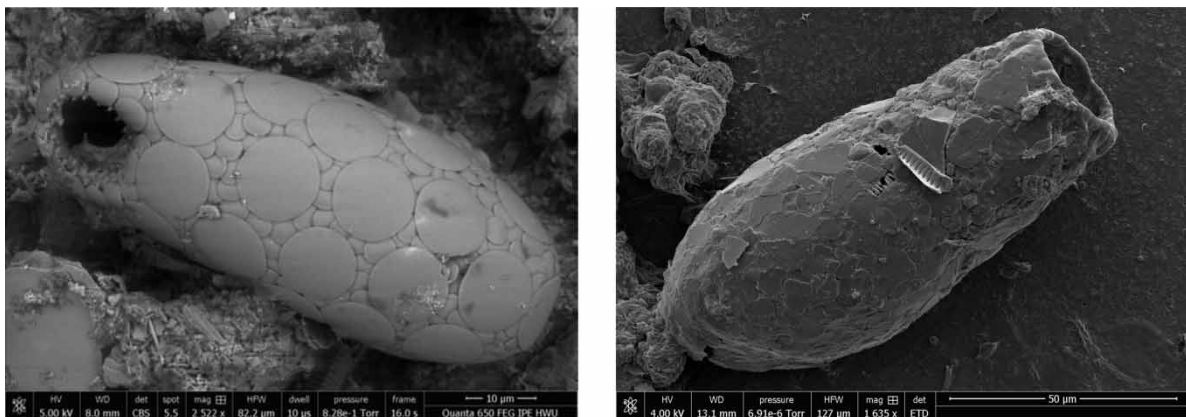


**Figure 3** | Examples of testate amoeba. Left: *Trinema* with shell made out of  $\text{SiO}_2$  circular plates. Right: *Diffflugia* with shell made out of silt-sized detrital silicate particles (quartz, feldspar).

Another kind of biological influence on SPM was observed in RBGE, where July samples revealed a number of faecal pellets rich in diatom detritus (Figure 4). Formation of these pellets would result in immediate removal of the entrained particles from the water column and is important for understanding both the SPM dynamics and biogeochemical cycling. Further indirect influences of invertebrates would have related to the fractionation of chemical elements due to shredding (Schaller *et al.* 2010).

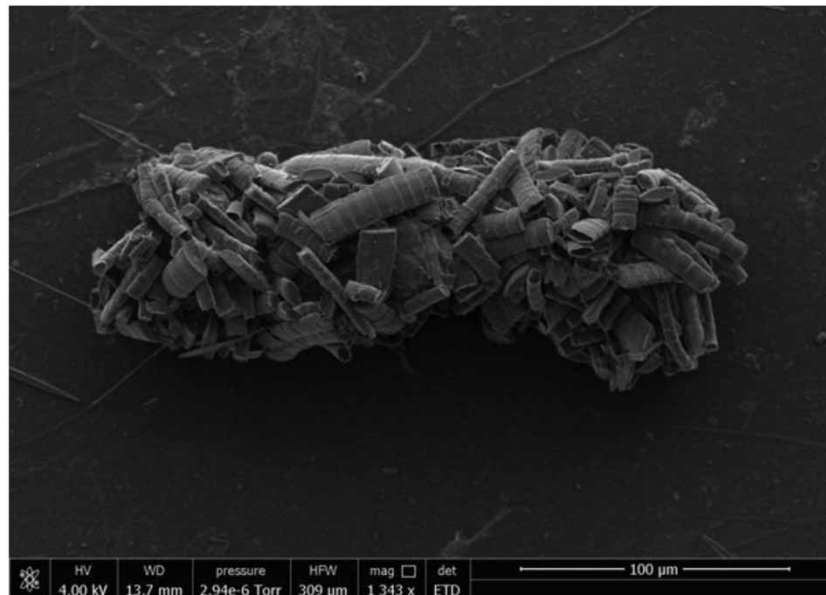


**Figure 4** | Example of a faecal pellet full of undigested diatom frustules (RBGE A July sample). The pellet is approximately 200 microns long.

## CHARACTERISATION OF SEDIMENTS IN THE PONDS STUDIED

A limited number (due to costs and logistical constraints) of sediment samples have been collected in June 2018 for XRF and particle size analysis. In some cases, two samples (points A and B) from a pond were collected. However, for Inverleith, Gore Glen, and Eliburn sites collection of suitable samples from two points was not feasible and only one sample per pond was taken.

### Sediments PSD

The results of PSD revealed, that similar to the SPM samples, a considerable (and often the major) proportion of sediments sampled was represented by particles smaller than 100 microns. Generally, however, sediment samples were characterised by coarser particle sizes. Furthermore, there appeared to be no direct relationship between PSD spectra of sediment samples and SPM spectra in the overlying water at the time of sampling. It should be noted, however, that for logistical reasons the methods of analysis of sediment and SPM samples were different and were undertaken on different instruments at two different universities. In particular, the SPM particulates analysed contained organic fraction, whilst it was eliminated in the sediments using hydrogen peroxide prior to analysis. These differences in pre-treatment might have contributed to the observed differences in particle sizes.

Some of the ponds (e.g. Gore Glen) had unimodal sediment PSD spectra, but many had secondary shoulder peaks (e.g. Eliburn, Granton A), and some exhibited bimodal or even multimodal shape of the spectrum (RBGE, Blackford B, Granton B). The shape of the spectra may have reflected the

diversity of sources for sedimenting particulates, including inputs from the catchment, detritus originating within the pond, and biologically mediated precipitation of inorganic compounds (see below).

It should be noted that for the majority of those ponds where two sediment samples were taken, the PSD spectra obtained at both points seemed to bear some visual resemblance, but the relationship was not always clear cut. If the SPM settling dynamics were governed purely by physical processes, a decrease in particle sizes would be expected between inflow and outflow. Interestingly, however, for Appleton, Blackford, Oxgangs and Granton ponds the samples obtained away from the main inflow were coarser and were characterised by higher median diameters (Figure 5). This may relate to the biologically induced coprecipitation of mineral compounds (see below) observed, for example, at Granton and Oxgangs. It should be noted that smaller sediment particle sizes away from the inflow were not observed at Juniper Green and RBGE sites; however, the former is a very small pond, whilst the latter has elevated levels of turbulence close to the outflow due to recirculation of water via an ornamental feature uphill.

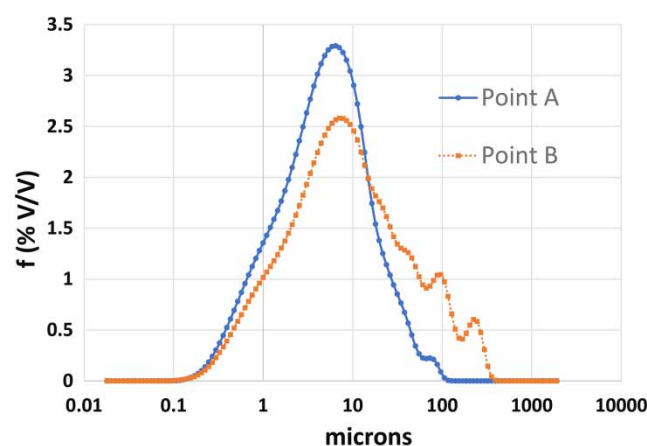


**Figure 5** | An example of PSD of bottom sediments. The samples were obtained from Appleton pond, close to inflow (Point A) and outflow (Point B).

An interesting feature was the presence of two shoulder peaks (one close to 100 microns, and another between 200 and 300 microns) in Appleton B, Eliburn and Granton spectra (Figure 5). The exact origin of these peaks is not clear and should be addressed by further research. It should also be noted that the sample from Inverleith pond (data not shown) was very different from all other samples. It was characterised by very coarse particle sizes; in fact, the spectrum was opened on the right and the mode was greater than the upper size limit of the technique. This sample was obtained close to the inflow point situated in a retrofitted constructed wetland; unfortunately, it was not possible to take a sample from the pond proper, as the cemented bottom of the pond is virtually lacking sediments presumably due to regular maintenance.

The high proportion of fine particles in the upper layer of sediments sampled has important implications for immobilisation of pollutants and biogeochemical cycling; the surface to volume ratio of fine particles is high, and so is the capacity for adsorption of nutrients and pollutants. That links well to the fact that a number of heavy metals and trace elements were found in these samples (see below). If grain size decreases, the content of adsorbed elements is expected to increase. The size of the sediment particles affects their entrainment, transport and deposition (Krivtsov *et al.* 2008a; Krivtsov *et al.* 2009) and therefore provides important clues to the sediment provenance, transport history and depositional conditions (see CIRIA780b and references therein). Grain size plays an essential role influencing the heavy metal contents in sediments; finer sediments contain more heavy metals than coarser ones, as the smaller grain size particles have a large surface-to-volume

ratio (Salomons & Förstner 1984; Martinčić *et al.* 1990). It should also be noted that the finer fraction of sediments may be easily resuspendable during times of high turbulence in windy weather, or following the disturbance by animals, or during high flow events. The resuspended fraction may be subsequently transported downstream via the outflow (Ahilan *et al.* 2019).

### Sediment chemistry

The most abundant elements in the sediment samples amongst those measured (Table 3) were Si (ranging between from just below 17% in Eliburn and Granton B samples to up to 28.73% at RBGE B sample, and Al (ranging between around 2.1–2.2% in RBGE and up to 12.43% in Appleton B sample). Both elements are widespread in the Earth's crust and are usually present in the lacustrine sediments (Krivtsov *et al.* 2001a). Interestingly, there was a weak positive correlation between Si and P whilst Al showed a negative relationship with P. These correlations suggest that the variable part of P pool was predominantly associated with organic material within diatoms, which are mainly composed of silicon.

Other elements routinely detected in the sediments in rather substantial quantities included Fe (2.84–10.06%), Ca (0.95–10.87%), S (0.17–3.65%), Mg (0.31–1.78%), K (0.43–1.21%), Na (0.27–1.82%), Ti (0.18–0.66%), P (non-detectable – 0.44%), Cl (0.005–0.75%) and Mn (0.053–0.21%). The presence of these elements is mostly similar to the SPM analysis (see below), although Ti in the SPM was seen only occasionally. In addition, such elements as Y and Cr were also detectable in the majority of bottom sediments, although Y and Cr were below the detection limit in the samples from RBGE pond. In contrast, Y and Cr in the suspended particulates were found only occasionally. Mo and Au, however, were not found in the sediment samples, although they were registered in some of the SPM samples. It should be noted, however, that Mo is difficult to separate from the much more abundant S using the method used; the results related to this element should therefore be treated with caution. Such pollutants as Co, Cu, Ni, Zn and As were detected in bottom sediments of all ponds.

Interestingly, P was undetectable in Gore Glen sediments. This pond experiences anoxia in the summer with epilimnion oxygen levels dropping to 3 ppm in June. The depletion of oxygen in the bottom layers is expected to be even greater (Krivtsov *et al.* 2001a; Krivtsov & Sigeo 2005) and may have led to the P release from sediments to the overlying water (Krivtsov *et al.* 2001b). Relatively low levels of P (0.054%) were also revealed for Oxgangs, another pond with very low water oxygen levels. However, even lower P values were observed for Appleton (0.048% for sample B) and there was no overall correlation between water oxygen or pH with sediment P. An attempt to apply a multiple regression (using oxygen and pH as predictive variables) was not successful either. Confounding factors might have been partly responsible for the absence of significant relationship of P with oxygen and pH. For example, Appleton pond water has a very high electrical conductivity value, and the pond is suspected to receive an illegal discharge from the upstream industries. The exact composition and temporal patterns of these inputs are unknown, and these should be investigated by further research.

### Elemental associations in bottom sediments

Pearson correlation analysis was used to reveal associations between various elements in the sediment samples and a summary of the results for the more abundant elements is given in Table 4. It showed an association among iron, aluminium and a large number of heavy metal pollutants, including Co, Cr, Ga, Gd, Ho, Rb, Tb, Ti, Y; this association will hereafter be referred to as A1. Magnesium and potassium also showed affinity to that association, revealing a significant correlation between themselves, aluminium and a number of relevant metals (Ga, Ti, Y). It should be noted that the dynamics of elements belonging to this association in the sediments will be largely governed by their chemical properties and abiotic factors, including T, pH, Eh, whilst biological factors are expected to be of secondary importance (Krivtsov & Sigeo 2005). However, the inorganic compounds

**Table 3** | Organic content (dwt%, estimated by loss on ignition – LOI) and chemical concentrations (mg/kg dwt) in the sediments of the ponds studied

| Ponds/Chemicals | Appleton | Blackford | Elburn  | Gore Glen | Granton | Inverleith | Juniper | Oxgangs | RBGE    |
|-----------------|----------|-----------|---------|-----------|---------|------------|---------|---------|---------|
| LOI             | 18       | 21.15     | 9.2     | 15.8      | 25.25   | 22         | 14      | 18.1    | 26.7    |
| Ac              | 5        | 5         | 5       | 20        | 5       | 10         | NF      | NF      | NF      |
| Ag              | 720      | 860       | 740     | 840       | 610     | 570        | 640     | 760     | 415     |
| Al              | 110,680  | 53,815    | 96,045  | 68,230    | 67,985  | 60,180     | 68,750  | 49,940  | 21,780  |
| As              | 5        | 25        | 10      | 10        | 10      | 10         | 20      | 10      | 10      |
| Ba              | 270      | 340       | 365     | 340       | 175     | 170        | 200     | 250     | 45      |
| Br              | 30       | 40        | 15      | 30        | 40      | 20         | 10      | 50      | 20      |
| Ca              | 10,905   | 62,980    | 32,190  | 21,250    | 25,575  | 13,970     | 12,010  | 108,680 | 13,755  |
| Ce              | 55       | 55        | 30      | 40        | 55      | NF         | 40      | 50      | 30      |
| Cl              | 5,470    | 215       | 110     | 90        | 1,075   | 440        | 380     | 3,230   | 895     |
| Co              | 255      | 200       | 195     | 250       | 200     | 110        | 120     | 180     | 125     |
| Cr              | 140      | 90        | 115     | 130       | 155     | 90         | 100     | 110     | NF      |
| Cs              | 5        | 20        | NF      | NF        | 5       | NF         | 10      | 10      | 5       |
| Cu              | 50       | 105       | 40      | 40        | 175     | 260        | 100     | 90      | 45      |
| Eu              | 190      | 160       | 165     | 290       | 165     | 150        | 110     | 70      | 185     |
| Fe              | 90,330   | 70,220    | 70,905  | 91,430    | 67,535  | 40,710     | 42,320  | 78,970  | 45,205  |
| Ga              | 30       | 10        | 20      | 10        | 20      | 10         | 10      | 10      | NF      |
| Gd              | 445      | 315       | 325     | 480       | 345     | 190        | 200     | 350     | 215     |
| Ho              | 50       | 5         | 15      | 30        | 15      | NF         | NF      | NF      | NF      |
| I               | 5        | 10        | 10      | 20        | 5       | NF         | NF      | 20      | 5       |
| K               | 11,550   | 7,440     | 11,645  | 9,420     | 10,960  | 8,170      | 10,640  | 5,010   | 4,830   |
| Mg              | 13,440   | 7,650     | 16,670  | 5,730     | 13,250  | 9,670      | 9,030   | 6,040   | 3,195   |
| Mn              | 570      | 1,255     | 1,035   | 2,060     | 690     | 920        | 590     | 1,190   | 1,345   |
| Na              | 9,760    | 10,140    | 11,185  | 3,750     | 7,830   | 8,530      | 9,300   | 6,480   | 2,235   |
| Nb              | 10       | 15        | 10      | 10        | 10      | 10         | 10      | 10      | NF      |
| Ni              | 35       | 85        | 85      | 30        | 45      | 20         | 30      | 20      | 80      |
| P               | 510      | 1,680     | 860     | NF        | 1,415   | 4,430      | 860     | 540     | 3,120   |
| Pa              | 15       | NF        | 5       | 10        | 5       | NF         | NF      | NF      | NF      |
| Pb              | 55       | 180       | 45      | 80        | 125     | 150        | 450     | 130     | 75      |
| Pm              | NF       | 25        | NF      | NF        | NF      | NF         | NF      | NF      | 110     |
| Pu              | NF       | 10        | 5       | 10        | NF      | NF         | NF      | NF      | NF      |
| Rb              | 90       | 60        | 80      | 70        | 60      | 30         | 50      | 50      | 15      |
| Re              | NF       | 5         | NF      | NF        | NF      | NF         | NF      | 10      | NF      |
| Sb              | 15       | 20        | 10      | 10        | 15      | 10         | 10      | 10      | 5       |
| Si              | 196,800  | 166,900   | 185,350 | 197,500   | 187,700 | 224,900    | 220,100 | 182,800 | 261,050 |
| Sm              | 15       | 20        | 10      | 20        | 10      | 10         | 10      | 30      | 20      |
| Sn              | 45       | 55        | 50      | 50        | 40      | 50         | 40      | 50      | 20      |
| S               | 10,600   | 15,200    | 1,700   | 36,500    | 17,450  | 9,700      | 3,700   | 25,500  | 30,550  |
| Sr              | 135      | 500       | 190     | 160       | 175     | 130        | 230     | 370     | 60      |
| Tb              | 805      | 575       | 590     | 720       | 580     | 270        | 350     | 630     | 280     |
| Te              | 25       | 35        | 25      | 30        | 20      | 20         | 20      | 30      | 10      |
| Th              | 10       | NF        | 10      | NF        | 5       | NF         | NF      | NF      | NF      |
| Ti              | 6,310    | 5,800     | 5,775   | 5,230     | 5,905   | 3,940      | 5,620   | 4,930   | 1,970   |
| V               | 165      | 145       | 100     | 90        | 160     | 60         | 80      | 150     | 55      |
| Y               | 25       | 30        | 25      | 20        | 20      | 10         | 20      | 20      | 5       |
| Zn              | 630      | 475       | 950     | 240       | 1,615   | 560        | 380     | 2,930   | 325     |

'NF' means that the element was below the detection limit of the XRF technique used. A number of elements (including At, Au, Bi, Cd, Dy, Er, Fr, Ge, Hf, Hg, In, Ir, La, Lu, Mo, Nd, Np, Os, Pd, Po, Pr, Pt, Ra, Rh, Ru, Sc, Se, Ta, Tc, Tl, Tm, U, W and Yb) were not detectable in any samples, and are therefore omitted from the Table.

**Table 4** | Summary of Pearson correlation analysis between elements in bottom sediments

| Chemical element | Negative Correlations   | Positive Correlations  |
|------------------|---|--|
| Si               | Ag, Ba, Ca, Cr, Nb, Rb, Sb, Sn, Sr, Tb, Te, Ti, V, Y, Zr        | <u>Pm</u> , P  |
| Al               | P, <u>Pm</u> , S  | Fe, Ba, Co, Cr, Ga, Gd, <u>Ho</u> , K, Mg, Pa, Rb, Tb, <u>Th</u> , Ti, Y |
| Fe               | P   | Al, Ag, Ce, Cl, Co, Cr, Ga, Gd, <u>Ho</u> , Rb, V, Y, Tb, Ti             |
| Ca               | Si  | <u>I</u>   |
| S                | K, Mg, Na, Ga, <u>Th</u> , Ti                                   | Mn   |
| Mg               | S, Mn, <u>Pm</u>  | Al, Cr, Ga, Pa, <u>Th</u> , Ti, Y, K                                     |
| K                | S, <u>Pm</u>  | Al, Ga, <u>Ho</u> , Rb, Ti, Y, Na, Mg                                    |
| Na               | <u>Pm</u>   | Ti, Mg, S  |
| Ti               | P, <u>Pm</u>  | Ag, K, Al, Ba, Co, Cr, Mg, Na, Fe, Ga, Gd, <u>Ho</u> , Nb                |
| P                | Al, Fe, Ag, Ba, K, Ga, Gd, Ho, Tb, Ti, V, Y, Ce, Co, Cr, Pa, Rb | <u>Si</u>  |
| Cl               | As  | Fe, Ga, Gd, <u>Ho</u> , Pa, Tb   |

The listed correlations are significant on the 95% probability level. Correlations significant on the 90% probability level are shown in italics. Underlined are the elements which were undetectable in large number of samples. Elements included in the statistical associations A1 and A2 are highlighted respectively in brown and green. See text for further details.

involved may be bound to the decaying organic matter – see [Krivtsov et al. \(2001a\)](#) and references therein.

Cl – the second most abundant cation registered by XRF – appeared to be associated with A1, revealing positive interactions with iron as well as Ga, Gd and Ho. However, S – the most abundant cation forming element registered by the method used – showed no affinity to the association A1. It revealed a number of negative relationships with the elements belonging to A1, whilst the only positive correlation of S was with Mn. Unlike Al and Fe, geochemical cycling of S in the sediments is more rapid and is directly biologically mediated – see [Zavarzin \(2008\)](#) and references therein. These differences between biological cycles are expected to be reflected in the correlation pattern observed.

Si was the most abundant element in the samples, and is also characterised by a biologically mediated cycle ([Krivtsov et al. 2000b](#)). Diatom algae use the dissolved silica to build their frustules, and many diatoms were observed among the suspended particulate matter in this research. A number of elements, including Ca, Mg, Al, Fe, S, Cl, Mn and P were registered in live diatoms by previous studies ([Krivtsov et al. 2000a, 2002b, 2003](#)). However, these elements tend to occur within the cells, and are not directly linked to the frustules. Following the cell death, some of these elements are leached out of the cell relatively fast.

The dissolution of frustules, however, is slow ([Krivtsov et al. 2001a](#)), and some of them contribute to the build-up of sediments ([Krivtsov et al. 2002a](#)). Statistical analysis on elemental concentrations in the cells of a diatom *Stephanodiscus rotula* in Rostherne Mere revealed a number of negative relationships between Si and other elements, which was interpreted as the absence of their association with silica frustules ([Krivtsov et al. 2003](#)). The results presented here revealed the scarcity of positive relationships of Si (although there was a sub-significant correlation with P), whilst many negative correlations were revealed. Therefore, it appears that the remains of diatom-derived Si frustules constitute a considerable proportion of the bottom sediments in the ponds studied.

P was the only major element correlated with Si. Biogeochemical cycles of Si and P in the aquatic environment are interdependent and linked through the dynamics of diatoms ([Krivtsov et al. 2000b](#)). Decomposition of P compounds may be relatively slow ([Krivtsov et al. 2001a](#)), which may explain the association between silica and phosphates (hereafter Association A2) revealed by our results.

Furthermore, there is chemical affinity of Si and P under conditions of neutral pH – see Schaller *et al.* (2019) and references therein. P therefore is expected to bind to the dissolving edges of partially decomposed diatom frustules (Schaller *et al.* 2019). Further evidence for the association of A2 comes from a similarity in correlation patterns revealed by both elements (Table 4).

#### Further analysis of elemental associations in bottom sediments using an enhanced dataset

To provide more information on the elemental associations in the bottom sediments, the dataset described above was combined with data from the Newcastle Great Park and J4M8 BGI ponds available from parallel research (Gogoi 2018); the detailed description of these locations is available elsewhere (Allen *et al.* 2017; Arthur *et al.* 2019). The combined dataset used for correlation analysis had 56 cases, which revealed the importance of particle size. Multivariate statistics using factor analysis (Table 5) were carried out to reveal relationships among the elements in sediments on a dataset containing 68 cases. The elements which had problems with missing values and/or insignificant concentrations were excluded from this analysis (e.g. Ge, Sc, Np, U, Pu).

The results of Spearman correlation analysis revealed a number of significant negative correlations between various sediment particle size measures (mean and median diameters, mode) and elemental concentrations of Al, V, Cr, Ce, Rb, Ga, Ho, Th and Pa. Although the correlation coefficients were relatively weak (typically in the range of 0.3–0.4), these elements showed affinity to smaller particle sizes. Adsorption of pollutants to small-sized sediment particles has been also documented by previous research – see Arthur *et al.* (2019) and references therein.

Visual analysis of the Scree plot (not shown) was used to limit the number of extracted factors to 5, which explained 73.2% of total variance. Extraction of further factors would have resulted in only a minor increase in the variance explained. The interpretation below will be based on the comparison of the factor loadings. The most abundant inorganic element in this dataset was Si and it showed association with Factor 1. The majority of other major elements (Al, Ca, Na and S) were also associated with only one factor. K and Fe, however, revealed association with two factors.

Factor 1 may be interpreted as aluminosilicates-based and is also enriched in Fe, K and Mg. A number of further elements showed an affinity to this factor, including Ac, Ag, Ce, Co, Cr, Ga, Gd, Ho, Nb, Rb, Sn, Tb, Te, Th, Ti, V, Y and Zr. It therefore appears that this factor might have reflected the influence of pollution, e.g. from weathering building materials.

Factor 2 may be interpreted as being associated with Fe and Mn compounds. It is also reflecting the influence of pollution, with such elements as Br, Co, Eu, Gd, Ni, Pm, Sm and Tb all having considerable loadings. Thus this factor appears to have reflected adsorption of REE and other trace elements to secondary minerals (Gosselin *et al.* 1992). Judging from the association with S, this factor may have also reflected the influence of cyclic changes in pH and oxygen conditions (Migaszewski & Gałuszka 2015); pyrite framboids were observed using SEM, for example, on Gore Glen samples following a drop in oxygen levels.

It should be noted that both Factor 1 and Factor 2 are likely to have also included biological influences. They both have high loadings on Fe and a number of trace elements. Trace elements, in particular REE, readily bind to organic materials as well as to the common Fe minerals like goethite (Migaszewski & Gałuszka 2015).

Factor 3 is related to calcite and also has high loadings on Re and Sr. Calcite was shown to be forming *in situ* by SEM studies (see above). It was implicated that Ca precipitation was bacterially mediated, and Factor 3 may be related to these processes. It does not appear to be associated with REE, possibly reflecting the low rate of their inclusion into the lattice due to the incompatibility of ionic radii (Steinmann & Stille 1997).

Factor 4 may be interpreted as being associated with decomposition of organic matter and coincident with elevated concentrations of sodium and potassium chlorides. Inputs of salts used for de-icing



**Table 5** | Results of factor analysis (absolute loadings >0.5) on sediment elements

|    | Component |       |       |       |       |
|----|-----------|-------|-------|-------|-------|
|    | 1         | 2     | 3     | 4     | 5     |
| Ac | 0.527     |       |       |       |       |
| Ag | 0.593     |       | 0.610 |       |       |
| Al | 0.850     |       |       |       |       |
| As |           |       | 0.575 |       |       |
| Ba |           |       |       |       | 0.863 |
| Br |           | 0.723 |       |       |       |
| Ca |           |       | 0.667 |       |       |
| Ce | 0.768     |       |       |       |       |
| Cl |           |       |       | 0.655 |       |
| Co | 0.782     | 0.517 |       |       |       |
| Cr | 0.885     |       |       |       |       |
| Cs |           |       | 0.577 |       |       |
| Cu |           |       |       |       |       |
| Eu |           | 0.638 |       |       |       |
| Fe | 0.744     | 0.573 |       |       |       |
| Ga | 0.804     |       |       |       |       |
| Gd | 0.749     | 0.573 |       |       |       |
| Hf |           |       |       | 0.757 |       |
| Ho | 0.670     |       |       |       |       |
| I  |           |       |       |       |       |
| K  | 0.566     |       |       | 0.602 |       |
| Mg | 0.605     |       |       |       |       |
| Mn |           | 0.508 |       |       | 0.680 |
| Na |           |       |       | 0.886 |       |
| Nb | 0.729     |       | 0.551 |       |       |
| Ni |           | 0.576 |       |       |       |
| P  |           |       |       |       | 0.721 |
| Pa |           |       |       |       |       |
| Pb |           |       |       |       |       |
| Pm |           | 0.686 |       |       |       |
| Rb | 0.834     |       |       |       |       |
| Re |           |       | 0.693 |       |       |
| Sb |           |       | 0.608 |       |       |
| Si | 0.518     |       |       |       |       |
| Sm |           | 0.653 |       |       |       |
| Sn | 0.612     |       | 0.599 |       |       |
| S  |           | 0.689 |       |       |       |
| Sr |           |       | 0.719 |       |       |
| Ta |           |       |       |       | 0.724 |
| Tb | 0.771     |       |       |       |       |
| Te | 0.521     |       | 0.586 |       |       |
| Th | 0.739     |       |       |       |       |
| Ti | 0.878     |       |       |       |       |
| V  | 0.803     |       |       |       |       |

*(continued)*

**Table 5** | continued

|    | Component |   |   |       |       |
|----|-----------|---|---|-------|-------|
|    | 1         | 2 | 3 | 4     | 5     |
| W  |           |   |   |       | 0.793 |
| Y  | 0.825     |   |   |       |       |
| Yb |           |   |   | 0.834 |       |
| Zn |           |   |   | 0.525 | 0.785 |
| Zr | 0.771     |   |   |       |       |

Extraction method: principal component analysis. Rotation method: Varimax with Kaiser normalization.

is the likely source of chlorides. Hf, Yb and Zn also appear to be associated with this factor. These elements might have been adsorbed to the surface of organic materials. Their presence also reflects the influence of pollution.

Factor 5 has association with Ba, Mn, P, Ta, W and Zn. Association with P is particularly important, as this element is likely to be limiting for biological production. The basis of this association may be related to precipitation of elements on geochemical barriers such as changes in pH and oxygen. Judging by the elemental composition, this association also reflects the influence of pollution.

It therefore appears that elemental associations revealed by factor analysis have resulted from a combination of processes related to the pollution sources, geochemical transformations within the system, and biological mediation. It should also be noted that the elemental association patterns derived from factor analysis on the enhanced dataset do not directly correspond to those derived using correlation analysis on the original dataset. For example, Factor 1 appears to have included A2 and a major part of association A1. Other parts of A1, however, appear to correspond to different factors. These differences reflect the fact that the enhanced dataset contains results from additional locations. Both sets of analysis have been helpful for interpretation of the patterns observed, and the results obtained should therefore be treated as complementary.

## DISCUSSION AND CONCLUDING REMARKS

There were more elements detected in sediments than in SPM and, generally speaking, most elements were present in higher quantities in sediments compared to SPM. This is due to the fact that the biologically derived organic fraction constituted the major part of SPM, whilst in the sediments it ranged between 9.2 and 33.7%. It should also be noted that the detection limits of the XRF technique used for the analysis of sediments is much lower than the detection limit of the SEM EDX method used for SPM (0.001 and 0.1% respectively). Hence the elemental concentrations in between these thresholds would be detectable in sediments but undetectable in SPM.

The results presented here have advanced the understanding of characteristics of suspended and sedimented particulate matter in BGI ponds, and implicated a number of physical, chemical and biological processes in influencing the patterns observed. Further studies should aim to elucidate fine details of these processes and, in particular, aim to shed further light on similarities and differences between SPM and bottom sediments, as well as among specific sites.

### Statistical associations of elements and the importance of biological processes

Elemental associations derived from statistical relationships help to enhance our understanding of the occurrence and behaviour of these elements within the BGI ponds and in aquatic ecosystems in

general. This information is useful for understanding their sources and pathways. It should be noted that although there were some similarities, the factor loadings pattern was considerably different for SPM and sediments. Hydrological sorting, settling and resuspension, dissolution and precipitation, flocculation, bioaccumulation and re-compartmentalisation by biological organisms are the likely contributing processes which should be investigated by further research.

Particle size showed a number of significant negative correlations with chemicals in sediments, which is in line with previous studies – see [Arthur \*et al.\* \(2019\)](#) and references therein. For SPM, however, the number of such relationships was very limited. Flocculation of particles aided by biologically produced organic compounds ([Krivtsov \*et al.\* 2008b](#)) may be responsible for masking these interactions.

This research highlighted the importance of biological processes for characterisation of SPM in BGI ponds. Planktonic organisms and the compounds they exude appeared to contribute the major part of SPM, and the results implicated some details of their involvement in biogeochemical cycling of specific elements. Application of SEM and X-ray based analytical techniques was particularly useful in that respect, as it allowed a combination of micrograph observations and chemical analysis. That was particularly relevant to Ca, Si, S, P, Fe and Mn with evidence gathered both from statistical analysis and from direct observations.

#### Accumulation of elements in sediments and implications for multiple benefits provided by BGI

This study has clearly demonstrated accumulation of pollutants in sediments of BGI ponds. The benefits of these findings are two-fold. Firstly, they provide evidence that these BGI ponds give at least some protection for the downstream environment by retaining potentially harmful substances. Potential remobilisation of these pollutants during low oxygen conditions and high flow events should be addressed by further research. Secondly, our results open up a possibility of recuperating the valuable resources accumulated in bottom sediments. This is particularly relevant to REE, as their usage has recently been increasing rapidly in relation to the global supplies ([Humphries 2013](#)). Previous studies have suggested recovering metals, metalloids and REE from wetlands constructed to remove pollutants from industrial effluent ([Schaller \*et al.\* 2013](#)). Our results indicate that this strategy should be extended to also include BGI ponds. In particular, in the ponds studied, the levels of such important chemicals as Ce (up to 70 ppm), Eu (up to 290 ppm), Gd (up to 490 ppm), Tb (up to 890 ppm), and in some samples also Sm (up to 30 ppm), were in the range reported for wetlands treating industrial effluent ([Schaller \*et al.\* 2013](#); [Migaszewski & Gałuszka 2015](#)). The levels are remarkably higher than those reported from natural environment, for example by Prego and co-authors ([Prego \*et al.\* 2009](#)) for Eu (1.8 ppm) and Gd (7.3 ppm), and for Tb reported by Hannigan and co-authors ([Hannigan \*et al.\* 2010](#)) from Chesapeake Bay (1.02 ppm) and by Zhu and co-authors ([Zhu \*et al.\* 1997](#)) from river sediments in China (1.16 ppm).

It should be noted that previous studies used REE as tracers on NGP and J4M8 ponds, which were included in the enhanced dataset ([Allen 2017](#); [Allen \*et al.\* 2017](#)). However, the application of REE happened a few years ago, the REE were attached to very small particles and it was concluded that they had a limited residence time within the system ([Allen 2017](#)). Furthermore, the average levels of REE in our core dataset are higher than those derived from NGP and J4M8 ponds. Specifically, higher concentrations in Edinburgh ponds (where the REE were not previously applied in experiments) compared to the additional ponds were observed for Ce (41 vs 26 ppm), Eu (168 vs 115 ppm), Tb (545 vs 301 ppm), Sm (16 vs 10 ppm) and Gd (322 vs 184 ppm). Slightly higher concentrations were also observed for some other trace elements, e.g. Y (20 vs 19 ppm). Hence the elevated trace elements levels in our samples are not due to the previous contamination from scientific research but have reflected other sources.

The exact origin of the REE in the ponds' sediments remains uncertain and is likely to include multiple sources. Previous research identified positive anomalies of Eu and Tb in the airborne particulate matter which was linked to the manufacturing of electronics (Suzuki *et al.* 2011); high levels of these elements have also been found in our samples.

The REE may be transported in the aquatic environment bound to SPM or associated with dissolved organic matter (Albéric *et al.* 2000). Furthermore, REE can be bioaccumulated by plants – see, for example, Schaller *et al.* (2013) and references therein. These elements are readily adsorbed both to clay minerals and to Fe and Mn oxides, which are known to be important for their dynamics (Nesbitt 1979; Johannesson & Zhou 1999). Our results also show association of REE with these compounds. Further studies will be needed to provide more detailed information on the REE sources and their dynamics in BGI ponds.

It should be noted that in properly maintained ponds, the sediments should be occasionally dredged according to the maintenance schedule (Woods-Ballard *et al.* 2007). The removed materials are usually disposed of on a landfill site for a fee. There is no reason why they could not be sent to a processing factory instead of a landfill, but the practicalities of that would be subject to the logistics and costs. Further studies should investigate the economic feasibility for recovery of these valuable resources, and consider including it among other multiple benefits provided by BGI (Fenner 2017).

#### Further relevance to UFR and BGC framework

A combination of hydrological and biogeochemical processes is expected to result in vertical downward transport of sedimenting particles and associated chemicals under conditions of low flow (Krivtsov *et al.* 2002a). During high flow events, however, the sediments may act as a source of suspended particulates and a chemical flux upward through the water column and downstream via the outflow (Ammar *et al.* 2015; Ahilan *et al.* 2019). The results of our research provide information on a comprehensive range of chemicals as well as particle sizes. They may therefore prove invaluable for informing modelling studies aiming to account for sediment and chemical budgeting of lentic and slow flowing systems (Krivtsov *et al.* 2002a) and will be particularly relevant for applications to BGI ponds (Ahilan *et al.* 2019), where detailed budgets of most elements have not yet been considered. The correct accounting of this budgeting will subsequently be of use for improving design and management of SUDS and other BGI ponds, thus helping to achieve water quality improvements downstream.

The results presented here are also of relevance for understanding the factors affecting planktonic communities in BGI ponds, as they provide information on trace elements potentially limiting algal growth. Cyanobacteria have been previously recorded in stormwater ponds (Vincent & Kirkwood 2014); this leads to a concern that BGI ponds may harbour neuro- and hepato-toxins with severe negative consequences for water quality and public health (Codd 1984). Cyanobacterial dominance is more likely to occur in warm weather under hydrological conditions of low flow; its probability will depend on the combination of potentially limiting factors including the availability of trace elements (Krivtsov *et al.* 1999b). The data on trace elements in SPM and sediments presented here are important in that respect.

It should also be noted that the results presented here are of relevance for the wider UFR/BGC framework. A well-developed BGI, including SUDS and other urban ponds, is set to become a common feature both in the UK and worldwide (Brears 2018; D'Arcy *et al.* 2018; DeBarry 2019; Krivtsov *et al.* 2019a). It is therefore important to understand all the fine details of functioning of these assets in order to eliminate uncertainty as regards their performance and to increase their public acceptability (Arthur *et al.* 2019, Krivtsov *et al.* 2019a). Our study contributes towards this important goal.

## ACKNOWLEDGEMENTS

This study has been carried out within the BGC UFR project ([www.urbanfloodresilience.ac.uk](http://www.urbanfloodresilience.ac.uk)) and funded by the EPSRC grants EP/P004180/1 and EP/P003982/1. Alejandro Sevilla, Simon Kennedy, Tanya Bezginova, Heather Forbes and Cesare Pertusi are kindly thanked for their contributions to field work. Comments of reviewers helped to improve the manuscript.

## COMPETING INTERESTS

We have no competing interests.

## AUTHORS' CONTRIBUTIONS

Funding: CT and SA. Study design: VK, CT, SA, PG, JB. Field Work: VK, PG, WG, AC, SA. Lab Work: VK, JB, TN, PG, WG, AC. Data analysis: VK, AC, JB, WG, PG, TN. Discussion: all authors. Write up: VK, JB, TN, PG. Editing: VK, JB, TN.

## REFERENCES

- Ahilan, S., Guan, M. F., Wright, N., Sleight, A., Allen, D., Arthur, S., Haynes, H. & Krivtsov, V. 2019 [Modelling the long-term suspended sedimentological effects on stormwater pond performance in an urban catchment](#). *Journal of Hydrology* **571**, 805–818.
- Albéric, P., Voillier, E., Jézéquel, D., Grosbois, C. & Michard, G. 2000 [Interactions between trace elements and dissolved organic matter in the stagnant anoxic deep layer of a meromictic lake](#). *Limnology and Oceanography* **45** (5), 1088–1096.
- Allen, D. 2017 *Beyond the Design Event: Sediment Pollution Movement in SuDS*. PhD Thesis, Heriot-Watt University.
- Allen, D., Arthur, S., Haynes, H. & Olive, V. 2017 [Multiple rainfall event pollution transport by sustainable drainage systems: the fate of fine sediment pollution](#). *International Journal of Environmental Science and Technology* **14** (3), 639–652.
- Ammar, R., Kazpard, V., Wazne, M., El Samrani, A. G., Amacha, N., Saad, Z. & Chou, L. 2015 [Reservoir sediments: a sink or source of chemicals at the surface water-groundwater interface](#). *Environmental Monitoring and Assessment* **187** (9), 579.
- Arthur, S., Krivtsov, V. & Allen, D. 2019 *Blue-green Infrastructure – Perspectives on Water Quality Benefits*. CIRIA C780b, London.
- Brears, R. C. 2018 Blue-Green Infrastructure in Managing Urban Water Resources. *Blue and Green Cities*. Palgrave Macmillan, London, pp. 43–61.
- Brouwer, P. 2006 *Theory of XRF*. PANalytical BV, Almelo, The Netherlands.
- Busquets, A., Fornós, J. J., Zafra, F., Lalucat, J. & Merino, A. 2014 [Microbial communities in a coastal cave: Cova des Pas de Vallgornera \(Mallorca, Western Mediterranean\)](#). *International Journal of Speleology* **43** (2), 8.
- Codd, G. 1984 Toxins of freshwater cyanobacteria. *Microbiological Sciences* **1** (2), 48–52.
- D'Arcy, B. J., Kim, L.-H. & Maniquiz-Redillas, M. 2018 *Wealth Creation Without Pollution. Designing for Industry, Ecobusiness Parks and Industrial Estates*. IWAP, London.
- DeBarry, P. A. 2019 Addressing Italy's urban flooding problems through the holistic watershed approach by using blue/green infrastructure. *UPLanD-Journal of Urban Planning, Landscape & Environmental Design* **4** (1), 127–136.
- Dittrich, M. & Obst, M. 2004 [Are picoplankton responsible for calcite precipitation in lakes?](#) *AMBIO: A Journal of the Human Environment* **33** (8), 559–565.
- Fenner, R. 2017 [Spatial evaluation of multiple benefits to encourage multi-functional design of sustainable drainage in blue-green cities](#). *Water* **9** (12), 953.
- Fenner, R., O'Donnell, E., Ahilan, S., Dawson, D., Kapetas, L., Krivtsov, V., Ncube, S. & Vercruyse, K. 2019 [Achieving urban flood resilience in an uncertain future](#). *Water* **11** (5), 1082. <https://doi.org/10.3390/w11051082>.
- Gogoi, P. 2018 *Impact Investigation of SUDS: Newcastle Great Park and J4M8 Distribution Park Edinburgh*. Nottingham University.
- Gosselin, D. C., Smith, M. R., Lepel, E. A. & Laul, J. 1992 [Rare earth elements in chloride-rich groundwater, Palo Duro Basin, Texas, USA](#). *Geochimica et Cosmochimica Acta* **56** (4), 1495–1505.
- Hannigan, R., Dorval, E. & Jones, C. 2010 [The rare earth element chemistry of estuarine surface sediments in the Chesapeake Bay](#). *Chemical Geology* **272** (1–4), 20–30.
- Hong, S., Soyol-Erdene, T.-O., Hwang, H. J., Hong, S. B., Hur, S. D. & Motoyama, H. 2012 [Evidence of global-scale As, Mo, Sb, and Tl atmospheric pollution in the antarctic snow](#). *Environmental Science & Technology* **46** (21), 11550–11557.

- Humphries, M. 2013 *Rare Earth Elements: the Global Supply Chain*. Congressional Research Service, Washington, DC.
- Johannesson, K. H. & Zhou, X. 1999 Origin of middle rare earth element enrichments in acid waters of a Canadian High Arctic lake. *Geochimica et Cosmochimica Acta* **63** (1), 153–165.
- Krivtsov, V. 2004 Investigations of indirect relationships in ecology and environmental sciences: a review and the implications for comparative theoretical ecosystem analysis. *Ecological Modelling* **174** (1–2), 37–54.
- Krivtsov, V. 2008 Indirect effects in ecology. In: *Systems Ecology, vol. 3, Encyclopedia of Ecology* (S. E. Jørgensen & B. D. Fath, eds). Elsevier, Oxford, pp. 1948–1958.
- Krivtsov, V. & Sigee, D. C. 2005 Importance of biological and abiotic factors for geochemical cycling in a freshwater eutrophic lake. *Biogeochemistry* **74** (2), 205–230.
- Krivtsov, V., Bellinger, E. & Sigee, D. 1999a Modelling of elemental associations in *Anabaena*. *Hydrobiologia* **414**, 75–81.
- Krivtsov, V., Sigee, D., Corliss, J. & Bellinger, E. 1999b Examination of the phytoplankton of Rostherne Mere using a simulation mathematical model. *Hydrobiologia* **414**, 71–76.
- Krivtsov, V., Tien, C., Sigee, D. & Bellinger, E. 1999c X-ray microanalytical study of the protozoan *Ceratium hirundinella* from Rostherne Mere (Cheshire, UK): dynamics of intracellular elemental concentrations, correlations and implications for overall ecosystem functioning. *Netherlands Journal of Zoology* **49** (4), 263–274.
- Krivtsov, V., Bellinger, E. & Sigee, D. 2000a Changes in the elemental composition of *Asterionella formosa* during the diatom spring bloom. *Journal of Plankton Research* **22** (1), 169–184.
- Krivtsov, V., Bellinger, E., Sigee, D. & Corliss, J. 2000b Interrelations between Si and P biogeochemical cycles – a new approach to the solution of the eutrophication problem. *Hydrological Processes* **14** (2), 283–295.
- Krivtsov, V., Sigee, D. & Bellinger, E. 2001a A one-year study of the Rostherne Mere ecosystem: seasonal dynamics of water chemistry, plankton, internal nutrient release, and implications for long-term trophic status and overall functioning of the lake. *Hydrological Processes* **15** (8), 1489–1506.
- Krivtsov, V., Sigee, D. C., Bellinger, E. G. & Porteous, G. 2001b Determination of P release from Rostherne Mere sediment cores. *Acta Hydrochimica et Hydrobiologica* **29** (2–3), 111–117.
- Krivtsov, V., Bellinger, E. & Sigee, D. 2002a Water and nutrient budgeting of Rostherne Mere, Cheshire, UK. *Nordic Hydrology* **33** (5), 391–414.
- Krivtsov, V., Sigee, D. & Bellinger, E. 2002b Elemental concentrations and correlations in winter micropopulations of *Stephanodiscus rotula*: an autecological study over a period of cell size reduction and restoration. *European Journal of Phycology* **37** (1), 27–35.
- Krivtsov, V., Bellinger, E. & Sigee, D. 2003 Ecological study of *Stephanodiscus rotula* during a spring diatom bloom: dynamics of intracellular elemental concentrations and correlations in relation to water chemistry, and implications for overall geochemical cycling in a temperate lake. *Acta Oecologica-International Journal of Ecology* **24** (5–6), 265–274.
- Krivtsov, V., Gascoigne, J. & Jones, S. 2008a Harmonic analysis of suspended particulate matter in the Menai Strait (UK). *Ecological Modelling* **212** (1–2), 53–67.
- Krivtsov, V., Howarth, M., Jones, S., Souza, A. & Jago, C. 2008b Monitoring and modelling of the Irish Sea and Liverpool Bay: an overview and an SPM case study. *Ecological Modelling* **212** (1–2), 37–52.
- Krivtsov, V., Howarth, M. & Jones, S. 2009 Characterising observed patterns of suspended particulate matter and relationships with oceanographic and meteorological variables: studies in Liverpool Bay. *Environmental Modelling & Software* **24** (6), 677–685.
- Krivtsov, V., Arthur, S., Allen, D. & O'Donnell, E. 2019a *Blue-green Infrastructure – Perspectives on Planning, Evaluation and Collaboration*. CIRIA C780a, London.
- Krivtsov, V., Arthur, S., Buckman, J., Bischoff, J., Christie, D., Birkinshaw, S., Takezawa, K., Chamberlain, D. & Pereira, R. 2019b *Monitoring and Modelling SUDS Retention Ponds: Case Studies From Scotland*. ICONHIC2019, Chania, Greece.
- Krivtsov, V., Birkinshaw, S., Arthur, S., Knott, D., Monfries, R., Wilson, K., Christie, D., Chamberlain, D., Brownless, P. & Kelly, D. 2020 Flood resilience, amenity and biodiversity benefits of an historic urban pond. *Philosophical Transactions of the Royal Society A* **378** (2168), 20190389.
- Kulaksız, S. & Bau, M. 2011 Rare earth elements in the Rhine River, Germany: first case of anthropogenic lanthanum as a dissolved microcontaminant in the hydrosphere. *Environment International* **37** (5), 973–979.
- Kulaksız, S. & Bau, M. 2013 Anthropogenic dissolved and colloid/nanoparticle-bound samarium, lanthanum and gadolinium in the Rhine River and the impending destruction of the natural rare earth element distribution in rivers. *Earth and Planetary Science Letters* **362**, 43–50.
- Ma, J. & Singhirunusorn, W. 2012 Distribution and health risk assessment of heavy metals in surface dusts of Maha Sarakham municipality. *Procedia-Social and Behavioral Sciences* **50**, 280–293.
- Marsalek, J., Rochfort, Q., Grapentine, L. & Brownlee, B. 2002 Assessment of stormwater impacts on an urban stream with a detention pond. *Water Science and Technology* **45** (3), 255–263.
- Martinčić, D., Kwokal, Ž & Branica, M. 1990 Distribution of zinc, lead, cadmium and copper between different size fractions of sediments I. The Limski Kanal (North Adriatic Sea). *Science of the Total Environment* **95**, 201–215.
- Migaszewski, Z. M. & Galuszka, A. 2015 The characteristics, occurrence, and geochemical behavior of rare earth elements in the environment: a review. *Critical Reviews in Environmental Science and Technology* **45** (5), 429–471.
- Nelson, S. M., Roline, R. A., Thullen, J. S., Sartoris, J. J. & Boutwell, J. E. 2000 Invertebrate assemblages and trace element bioaccumulation associated with constructed wetlands. *Wetlands* **20** (2), 406–415.

- Nesbitt, H. W. 1979 Mobility and fractionation of rare earth elements during weathering of a granodiorite. *Nature* **279** (5710), 206.
- O'Donnell, E., Thorne, C., Ahilan, S., Arthur, S., Birkinshaw, S., Butler, D., Dawson, D., Everett, G., Fenner, R., Glenis, V., Kapetas, L., Kilsby, C., Krivtsov, V., Lamond, J., Maskrey, S., O'Donnell, G., Potter, K., Vercruyse, K., Vilcan, T. & Wright, N. 2020 The blue-green path to urban flood resilience. *Blue-Green Systems* **2** (1), 28–45.
- Oxford Instruments 2013 AZtec manual. Oxford Instruments NanoAnalysis, Oxford.
- Oxford Instruments 2019 Detection limits of the SEM-EDX method and treatment of statistical uncertainties in the analysis of trace elements (communication by email). Oxford Instruments NanoAnalysis, Oxford.
- Perelomov, L. & Kandeler, E. 2006 Effect of soil microorganisms on the sorption of zinc and lead compounds by goethite. *Journal of Plant Nutrition and Soil Science* **169** (1), 95–100.
- Perelomov, L. & Yoshida, S. 2008 Effect of microorganisms on the sorption of lanthanides by quartz and goethite at the different pH values. *Water, Air, and Soil Pollution* **194** (1–4), 217–225.
- Prego, R., Caetano, M., Vale, C. & Marmolejo-Rodríguez, J. 2009 Rare earth elements in sediments of the Vigo Ria, NW Iberian Peninsula. *Continental Shelf Research* **29** (7), 896–902.
- Reynolds, C. S. 1984 *The Ecology of Freshwater Phytoplankton*. Cambridge University Press, Cambridge.
- Reynolds, C. S. 2006 *The Ecology of Phytoplankton*. Cambridge University Press, Cambridge.
- Salomons, W. & Förstner, U. 1984 *Metals in the Hydrocycle*. Springer-Verlag, Berlin, Heidelberg New York, p. 349.
- Schaller, J., Weiske, A., Mkandawire, M. & Dudel, E. G. 2010 Invertebrates control metals and arsenic sequestration as ecosystem engineers. *Chemosphere* **79** (2), 169–173.
- Schaller, J., Vymazal, J. & Brackhage, C. 2013 Retention of resources (metals, metalloids and rare earth elements) by autochthonously/allochthonously dominated wetlands: a review. *Ecological Engineering* **53**, 106–114.
- Schaller, J., Faucherre, S., Joss, H., Obst, M., Goeckede, M., Planer-Friedrich, B., Peiffer, S., Gilfedder, B. & Elberling, B. 2019 Silicon increases the phosphorus availability of Arctic soils. *Scientific Reports* **9** (1), 449.
- Sörme, L. & Lagerkvist, R. 2002 Sources of heavy metals in urban wastewater in Stockholm. *Science of the Total Environment* **298** (1–3), 131–145.
- Steinmann, M. & Stille, P. 1997 Rare earth element behavior and Pb, Sr, Nd isotope systematics in a heavy metal contaminated soil. *Applied Geochemistry* **12** (5), 607–623.
- Sternbeck, J., Sjödin, Å. & Andréasson, K. 2002 Metal emissions from road traffic and the influence of resuspension – results from two tunnel studies. *Atmospheric Environment* **36** (30), 4735–4744.
- Suzuki, Y., Hikida, S. & Furuta, N. 2011 Cycling of rare earth elements in the atmosphere in central Tokyo. *Journal of Environmental Monitoring* **13** (12), 3420–3428.
- Thorpe, A. & Harrison, R. M. 2008 Sources and properties of non-exhaust particulate matter from road traffic: a review. *Science of the Total Environment* **400** (1–3), 270–282.
- Tien, C. J., Krivtsov, V., Levado, E., Sigee, D. C. & White, K. N. 2002 Occurrence of cell-associated mucilage and soluble extracellular polysaccharides in Rostherne Mere and their possible significance. *Hydrobiologia* **485** (1–3), 245–252.
- van Leeuwen, H. P. & Buffle, J. 2009 Chemodynamics of aquatic metal complexes: from small ligands to colloids. *Environmental Science & Technology* **43** (19), 7175–7183.
- Vincent, J. & Kirkwood, A. E. 2014 Variability of water quality, metals and phytoplankton community structure in urban stormwater ponds along a vegetation gradient. *Urban Ecosystems* **17** (3), 839–853.
- Wei, B. & Yang, L. 2010 A review of heavy metal contaminations in urban soils, urban road dusts and agricultural soils from China. *Microchemical Journal* **94** (2), 99–107.
- Woods-Ballard, B., Kellagher, R., Martin, R., Jefferies, C., Bray, R. & Shaffer, P. 2007 *The SuDS Manual*. CIRIA C697, London.
- Zafra, C., Temprano, J. & Suárez, J. 2017 A simplified method for determining potential heavy metal loads washed-off by stormwater runoff from road-deposited sediments. *Science of the Total Environment* **601**, 260–270.
- Zavarzin, G. 2002 Microbial geochemical calcium cycle. *Microbiology* **71** (1), 1–17.
- Zavarzin, G. A. 2008 Microbial cycles. In: *Encyclopedia of Ecology* (Jorgensen, S. E. & Fath, B. D., eds). Newnes, pp. 2335–2347.
- Zayed, A., Gowthaman, S. & Terry, N. 1998 Phytoaccumulation of trace elements by wetland plants: I. Duckweed. *Journal of Environmental Quality* **27** (3), 715–721.
- Zhu, W., Kennedy, M., De Leer, E., Zhou, H. & Alaerts, G. 1997 Distribution and modelling of rare earth elements in Chinese river sediments. *Science of the Total Environment* **204** (3), 233–243.

First received 5 February 2020; accepted in revised form 26 March 2020. Available online 30 May 2020